Available online at www.sciencedirect.com

ScienceDirect

journal homepage: www.elsevier.com/locate/he

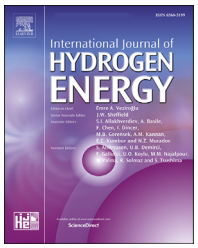

Performance analysis of a novel heat recovery system with hydrogen production designed for the improvement of boiler effectiveness

Oguz Arslan

Thermodynamics Division, Mechanical Engineering Department, Engineering Faculty, Bilecik Seyh Edebali University, Bilecik, 11230, Turkey

HIGHLIGHTS

- A novel system with hydrogen production is designed for the waste heat recovery.
- An exergy efficiency increase of 8.49% for air enriched case is achieved.
- An exergy efficiency increase of 2.45% for air and fuel enriched case is achieved.
- A decrease about 2.35% in the fuel consumption is achieved.

ARTICLE INFO

Article history:
Received 12 October 2020
Received in revised form
25 November 2020
Accepted 27 November 2020
Available online 28 December 2020

Keywords:
Coal-fired boiler
Exergy
Enriched air combustion
Hydrogen production
Bottoming cycle
Waste heat

ABSTRACT

In this study, a multi-generation system is designed for the waste recovery of a 150 MW coal-fired power plant. The waste heat from the boiler system of the power plant is recycled in the power block with supercritical organic Rankine Cycle to obtain the required energy for the proton exchange membrane electrolyzer block. Then, two different cases are handled to utilize the products of the proton exchange membrane electrolyzer block. In the first case, H_2 is stored as an energy carrier to be used for external operations where O_2 was used for the enrichment of the combustion air. In the second case, H_2 is used for the enrichment of the fuel where O_2 is used for the enrichment of the combustion air as in the first case. It is determined that it is available to produce H_2 in an amount of 0.0417 −0.0433 kmol/s. The energy efficiency of the overall system is determined as 25.37% and 24.05% where the exergy efficiency of the overall system is determined as 31.56% and 29.80% for the first and second cases, respectively.

Introduction

Coal as an energy source has considerable use for power generation despite its emissions to the environment. So that, in Turkey, 22.4% of total electricity generation is provided by coal-fired power plants in which lignite with low heating value is commonly used [1]. Since there is no chance to give up this kind of plant with the old technologies, the new solutions are urgently needed to improve the performances of these plants for environmental issues. In this regard, the boiler seems the most critical component to be improved from the environmental point of view [2–4]. In this regard, the most effective solutions is to improve the combustion process and/or to

E-mail address: oguz.arslan@bilecik.edu.tr.
https://doi.org/10.1016/j.ijhydene.2020.11.253

evaluate the waste heat of the flue-gases since there is still a lot of energy to use, even if temperature is not so high as working fluid temperature [5,6]. There are limited solutions in this aim which include mainly of the three ways. The first one is to recuperate the components of the boiler such as nozzles and heat exchangers. The second one is the flotation of the fuel. The third one, which is the main aim of this study, is to improve the combustion air for a better reaction.

Depending on the combustion nature, it is the best way to increase the oxygen (O_2) amount of the combustion air to improve the process since it prevents the energy losses caused by the excess air. In the combustion process, a considerable amount of the produced energy is wasted to heat the nitrogen (N_2) of the combustion air. So, the increase in the amount of O_2 would decrease the ratio of N_2 in the combustion air. This operation would also decrease the amount of required excess air for a better mixing of fuel and air which means higher efficiency [7,8]. In this regard, oxy enriched combustion (OEC) and oxy-fuel combustion have attracted more attention to the higher efficient combustion process and lower emissions [9,10]. Horbaniuc et al. [11], in their study, investigated OEC in supercritical steam boilers and reported an increase of up to % 5 in the boiler's efficiency. Tiwari et al. [12] reported a combustion efficiency of 93.8% with an O_2 rate of 31%. This means an efficiency increase of about 5% for combustion efficiency. Zhan et al. [13] reported an energy efficiency improvement of 2.2% for the boiler when the O_2 volume in the atmosphere is 29%. Yu et al. [14] reported an increase in a rate of 6% in the combustion efficiency when the O_2 enriched air and standard air are compared. However, the pure O_2 is needed to obtain the enriched combustion air. Two common methods, namely distillation, and adsorption are usually used to obtain pure O_2. Electrolysis also can be taken into account as a method of producing pure O_2 although the main aim of the process is to produce H_2. The electrolysis way of H_2 production mainly has three kinds of technologies including alkaline electrolyzer (AEL), proton exchange membrane electrolyzer (PEMEL) with an acidic polymer membrane used as a solid electrolyte, and high-temperature electrolyzer (HTEL) with a solid oxidizer used as electrolyte [15].

However, in comparison to other methods, electrolysis is a more expensive way since it needs an external heat and electricity source. But, the production of H_2 —as an efficient energy carrier and attractive energy storage medium-makes electrolysis more advantageous from the energy efficiency point of view [16]. If the external energy need is satisfied by a free source, then electrolysis would be more attractive for the energy systems. The renewables are commonly used as free energy sources, and several systems were conducted for this aim in the literature. Bicer and Dincer [17] developed a new hybrid system for H_2 production using solar and geothermal sources. They conducted energy and exergy efficiency up to 10.8% and 46.3%, respectively. The produced H2 was determined as 0.11 kg/h. Bamisile et al. [18] performed a new solar Parabolic Trough Collector (PTC) integrated system for the multi-generation purpose. One of the multi-generation products was H2 obtained through a PEMEL. They reported an H_2 production rate of 0.9785 kg/h from the designed system. They also reported a reduction of CO_2 in the amount of 768.85 kg/h based on using fuel oil. Safari and Dincer [19] investigated H_2 and methane (CH_4) production through a comprised system of a wind turbine, PEMEL, and a methanation unit. They conducted a new design for CO_2 capture by the methanation process in which the produced H_2 was used. They reported an H_2 production rate of 0.4131 kg/h which resulted in a CO_2 capture of 2.176 kg/h. Balta et al. [20] investigated geothermal energy based H_2 production through the HTEL. They conducted overall energy and exergy efficiency of 87% and 86%, respectively. Besides, they reported the H_2 production amount as 573 mol/s with electricity consumption of 3.34 kWh. Omar and Altinisik [21] simulated H_2 production by electrolysis unit integrated with a solar collector. According to the simulation, it is available to produce H_2 in the amount of 16 kg for the selected region. Seyitoglu et al. [22] investigated H_2 production by coal gasification. They handled the HTEL system fed by the Brayton cycle, the steam Rankine cycle (STR), an organic Rankine cycle (ORC). They reported the energy and exergy efficiency of the system as 41% and 36.5%, respectively. The reported H_2 changes between 1.7 and 2.4 kg/s for the handled different coal types. Gokcek and Kale [23] designed a PEMEL H_2 production system with a capacity of 125 kg/d. The handled system was powered by wind and photovoltaic (PV) hybrid system. Yilmaz et al. [24] designed a combined plant base on concentrating solar collectors for poly-generation purposes. One of the aims of the study was H_2 production by PEMEL. They reported an H_2 amount of about 0.0682 kg/s with an energy and exergy efficiency of 62.53% and 58.68%, respectively. Fereidooni et al. [25] conducted a comprehensive study on H_2 production from PV station. They conducted an H_2 production rate of 56 tons per month (August) by electricity consumption of 3465 kWh. The studies showed that PEM cells were profitable when they were used as thermolelectric generator aided by waste heat [26–28]. It is also available to evaluate the waste heat for H_2 production. Lummen et al. [29] investigated H_2 production by the waste heat of condensing steam. They used a PEMEL stack for this purpose. They conducted that it was possible to obtain H_2 production of 1.27 g per unit steam with a reduction of 30% in waste heat rejection. Nami et al. [30] proposed an integrated system for H_2 and power generation. The coupled the PEMEL with Turbine Modular Helium Reactor/Organic Rankine Cycle (GTMHR/ORC) system. They conducted an H_2 production rate of 56.2 kg/h with an exergy efficiency of 49.21%. Feili et al. [31] proposed a novel trigeneration system working with waste heat of the marine diesel engine. The trigeneration system was formed of ORC, PEMEL and cooling cycle. They conducted that it was available to achieve an exergy efficiency uo to 18.71% with an H_2 production of 0.33 kg/h. Thiyagarajan et al. [32] investigated H_2 production by the waste heat of exhaust gas of a compressed ignition engine. In the study, they used the exhaust gas in thermoelectric module to generate power. The generated power was then used in a PEMEL to produce H_2. Finally, the produced H_2 was inducted to the engine to improve the efficiency. They conducted a brake thermal efficiency improvement of 10%.

In this study, a novel hybrid system was designed to improve boiler efficiency. The system includes a PEMEL and an ORC system integrated into a coal-fired power plant. Two cases were handled in the study. For the first case, the produced H_2 is fed to the boiler system to enrich the fuel where O_2

is mixed with the air to enrich the combustion air. For the second case, the produced H_2 is stored in a high-pressure tank to be evaluated for different aims where O_2 is mixed with the air to enrich the combustion air again. PEMEL is powered by an ORC system to recover the waste heat of stack gases. The designed system was evaluated by the energy and exergy method to measure the performance. Finally, the system was evaluated from an environmental point of view.

System description

Seyitomer coal-fired power plant serves to generate electricity with its old-fashion technology. The plant has a capacity of 600 MW including four units in which one of the units is out of order now. In this study, the latest built one has been into consideration. The unit has an air preheating system with an output temperature of flue gases ranging between 285 and 305 °C. Thereby, a large amount of waste heat is available to recover. In this aim, a novel hybrid system was designed to recover the waste heat and to improve boiler efficiency. The flowchart of the designed hybrid system is given in Fig. 1.

According to this hybrid system, the waste heat is used in a supercritical-ORC unit to generate electricity which feeds a PEMEL unit. The secondary product (O_2) of PEMEL is used to enrich the combustion air for improving the combustion efficiency where the main product (H_2) is stored in a high-pressured tank for an energy carrier (Case-I) or is used to enrich the fuel for better combustion process (Case-II, dashed line in Fig. 1). The new design consists of three main structures namely boiler group (BG), hydrogen electrolyzer group (PEMEL Block), and ORC power block. BG mainly consists of air preheater (APH) and boiler (B). The boiler includes four main components namely the combustion chamber, heater, superheater, and economizer. In this study, the effects on the combustion chamber were handled and the operation conditions were kept constant to observe the improvements. A large part of the waste heat from BG is used in ORC where remained small part is used for the heat demand of the electrolyzer to obtain the required heat. ORC has four main components namely evaporator (E), turbine group including generator (T), condenser (Con), and pump (P1). The generated electricity in ORC is used for the energy demand of the electrolyzer. PEMEL block is mainly formed of heat exchanger (HE-

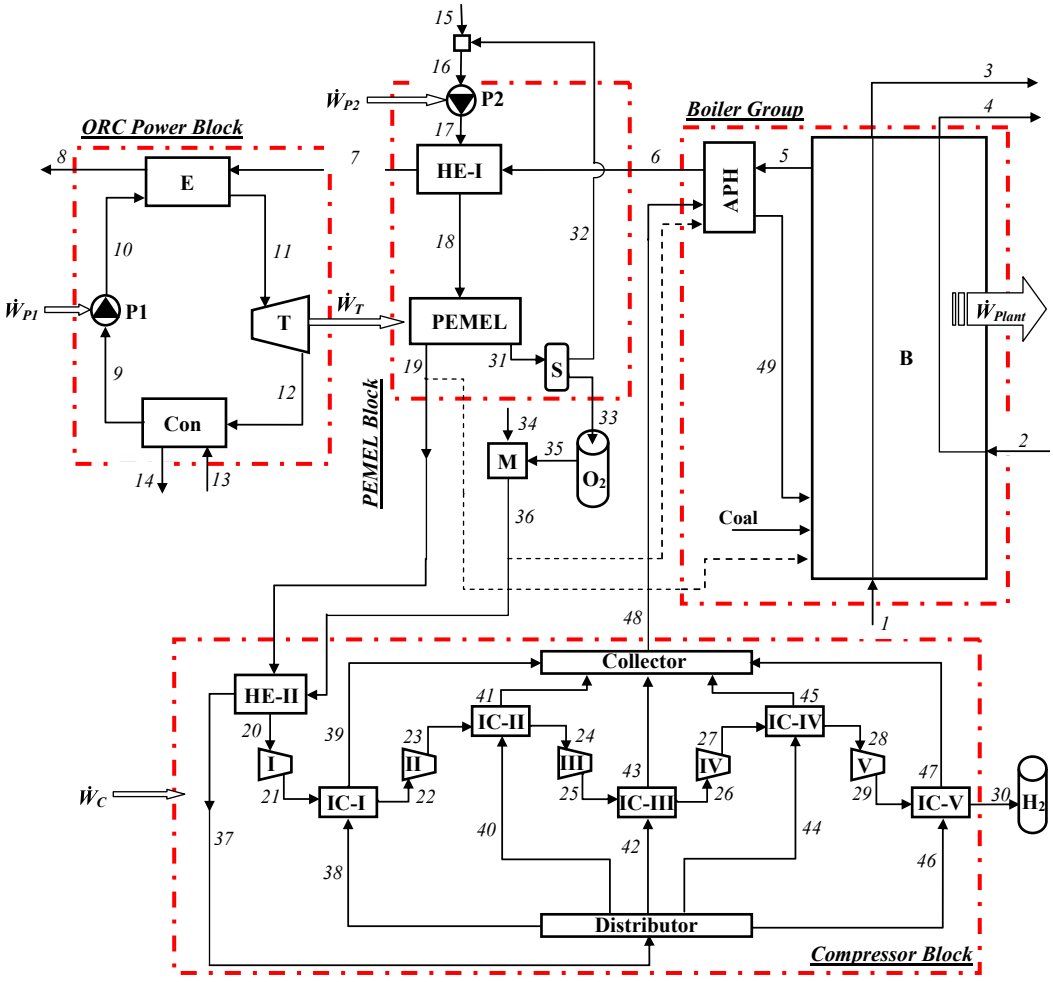

Fig. 1 – Flow diagram of the proposed system.

1), proton exchange membrane electrolyzer stack (PEMEL), compressor block (CB), separator (S), pump (P2), and storage tanks. The compressor block is just used when the Case-I am taken into account. In this case, the compressor block is handled as five staged to decrease the required power. The heat generated in the block is recovered to improve boiler efficiency.

Thermodynamic analysis

Three main structures namely the boiler group, PEMEL, and ORC were taken into account for the thermodynamic analysis. Then these structures were evaluated by the exergy method taking the overall system into account. An exergy analysis is conducted in conjunction with the continuity of mass and the first law of thermodynamics. The mass, energy, and exergy balance equations for the steady-state conditions are orderly given as follows [33,34]:

$$\sum \dot{m}_i - \sum \dot{m}_o = 0 \tag{1}$$

$$\dot{Q} - \dot{W} + \sum \dot{m}_i h_i - \sum \dot{m}_o h_o = 0 \tag{2}$$

$$\dot{E}x_{d,k} = \dot{E}x_k^Q - \dot{E}x_k^W - \sum \left(\dot{m}_i ex_i\right)_k - \sum \left(\dot{m}_o ex_o\right)_k \tag{3}$$

where $\dot{Q}$ is heat rate term, $\dot{W}$ is work term, $\dot{m}$ is the mass rate. i indicates the inlet conditions and o indicates the outlet conditions. $\dot{E}x_{d,k}$, $\dot{E}x_k^Q$, $\dot{E}x_k^W$ and ex respectively describe the destructed exergy, the exergy of heat energy, the exergy of work and the specific exergy of flow, and are given as:

$$\dot{E}x_k^Q = \left(1 - \frac{T_0}{T}\right)\dot{Q}_k \tag{4}$$

$$\dot{E}x_k^W = \dot{W}_k \tag{5}$$

$$ex_i = ex_i^{Ph} + ex_i^{Ch} \tag{6}$$

where ex_k^{Ph} is the physical exergy term and is given by:

$$ex_i^{Ph} = (h_i - h_0) - T_0(s_i - s_0) \tag{7}$$

or

$$ex_i^{Ph} = c_p\left(T_i - T_0 - T_0 \cdot \ln\left(\frac{T_i}{T_0}\right)\right) \tag{8}$$

If the process includes a chemical reaction in itself, then the chemical term should be taken into account where is given by:

$$ex_{ch} = \sum_i x_i ex_{i,ch} + R_u T_0 \sum_i x_i \ln(x_i) \tag{9}$$

here, h and s indicate orderly the enthalpy and entropy at a certain state. c_p is the specific heat of gas-phase flow. Subscript of 0 indicates the reference state conditions which are taken as 25 °C and 1 atm in this study. P is the total pressure of the stream, x_i is the mole fraction, and $ex_{i,ch}$ standard chemical exergy of the ith substance. So, energy efficiency (η), exergy efficiency (ε), and exergy destruction ratios (y) are respectively given as:

$$\eta = \frac{\dot{E}_{o,k}}{\dot{E}_{i,k}} \tag{10}$$

$$\varepsilon = 1 - \frac{\dot{E}x_{d,k}}{\dot{E}x_{i,k}} \tag{11}$$

$$y_k = \frac{\dot{E}x_{d,k}}{\dot{E}x_{i,total}} \tag{12}$$

The chemical exergy values were obtained from Ref. [34]. The energy and exergy efficiencies of PEMEL block is calculated using the low heating value (LHV) and chemical exergy values of H_2 where they are taken as 240,000 kJ/kmol and 236,000 kJ/kmol, and are given as follows:

$$\eta = \frac{\dot{n}_{H2} LHV}{\dot{W}_{PEMEL}} \tag{13}$$

$$\varepsilon = \frac{\dot{n}_{H2} ex_{H2,ch}}{\dot{W}_{PEMEL}} \tag{14}$$

Boiler group-BG

The boiler group (BG) is formed of the boiler (B) and the air preheater system (APH). In the thermodynamic evaluation of BG, the output values of the real (measured) case were preserved to compare the case effectively. The handled unit of Seyitomer plant is fed with the low-calorific lignite with high moisture and ash content about 31.5% and 47.34% by weight in order. The elemental analysis of the lignite is given in Table 1 [35].

As mentioned in the section system description, three different cases were formed. The first case is the base case which the process already goes on. The products of the base combustion process were measured in-situ for the handled steam cycle unit. The unmeasured values were determined through Eq. (1) taking into account the mass balance. The

Table 1 – Elemental analysis of the Seyitomer lignite.

Compound	wt%	kmol/kg-lignite (af)		
		Base	Case I	Case II
C	13.66	0.0113810	0.0113810	0.0113810
S	0.54	0.0001701	0.0001701	0.0001701
N	0.03	0.0000120	0.0000120	0.0000120
O	4.07	0.0012708	0.0012708	0.0012708
H	2.86	0.0142992	0.0142992	0.0148940
Moisture	31.50	0.0174991	0.0174991	0.0174991
Ash	47.34	–	–	–

$$\overbrace{(C+H+N+S+O+H_2O_{(fluid)})}^{Fuel}+\lambda\cdot a\cdot\overbrace{(3.76\cdot N_2+O_2)}^{Air}\rightarrow\overbrace{b\cdot CO+c\cdot CO_2+d\cdot NO_2+e\cdot SO_2+f\cdot O_2+g\cdot N_2+h\cdot H_2O_{(gaseous)}}^{Products} \quad (15)$$

technical characteristics of measurement equipment are given in Table 2 [36].

Here, the term "*a*" indicates the coefficient of combustion air for the stoicheiometric condition where λ indicates the coefficient of excess air.

In the second case (Case I), the obtained H_2 from PEMEL is stored as an energy carrier where O_2 is fed to the boiler for the enrichment of combustion air. In the third case (Case II), the product H_2 of PEMEL is fed to the boiler for the enrichment of fuel where O_2 is fed to the boiler for the enrichment of combustion air as in Case I. In all cases, the excess air was kept the same as in the base case for better comparison. In Case II, the required air for the complete combustion process of H_2 is calculated with the assumption of 10% excess air. In this regard, the molar rates of the reactants were calculated (see Table 1) and the combustion reactions were formed according to Eq. (1). The coefficients of combustion products are given in Table 3.

In the terms of reactants and products, the heat obtained from the combustion reaction is given by the following equation [33]:

$$\dot{Q}_f=\sum_i\dot{n}\left(\overline{h}_0^f-\overline{h}_T-\overline{h}_{298}\right)-\sum_o\dot{n}\left(\overline{h}_o^f-\overline{h}_T-\overline{h}_{298}\right) \quad (16)$$

where, $\dot{Q}_f$ describes the heat of fuel. $\dot{n}$, $\overline{h}_0^f$, $\overline{h}_T$ and $\overline{h}_{298}$ are the mole ratio, molar enthalpy of formation, molar enthalpy at the temperature *T*, and molar enthalpy at 298 K, respectively. So, the exergy of the combustion process can be obtained by the following equation [34,37]:

$$\dot{E}x_f=\left(1-\frac{T_0}{T_{cc}}\right)-I \quad (17)$$

where T_{cc} indicates the temperature of the combustion chamber assumed as adiabatic combustion temperature. The term.; *I* describes the exergy destruction rate and is given as in terms of generated entropy (S_g) and reference state temperature ($T_0 = 298$ K) [33]:

$$I=\dot{E}x_{d,f}=T_0S_g \quad (18)$$

$$S_g=S_o-S_i+\frac{\dot{Q}_f}{T_{cc}} \quad (19)$$

where, S_o, an S_i respectively define the entropies of reactants and products which is calculated by the following equation [33]:

$$S_k=\sum_o\dot{n}_k\left(\overline{s}_k^o(T,P_0)-R_u ln(x_kP)\right) \quad (20)$$

Here, $\overline{s}_i^o$, R_u , x_k and *P* are orderly absolute molar entropy of the *k*th component, universal gas constant, mole ratio of the *k*th compound, and total pressure of the flow.

Table 3 – Coefficients of combustion balance for ash-free lignite.

Compound		*n* (kmole/kg-lignite)		
		Base	Case I	Case II
Air	λ	1.680	1.671	1.668
	a		0.0274623	
CO_2	b	0.0108745	0.0108745	0.0108745
CO	c	0.0005065	0.0005065	0.0005065
SO_2	d	0.0001701	0.0001701	0.0001701
NO_2	e	0.0000120	0.0000120	0.0000120
N_2	f	0.1734737	0.1725030	0.1722449
O_2	g	0.0289500	0.0289500	0.0286229
$H_2O_{(gaseous)}$	h	0.0317983	0.0317983	0.0323930

Table 2 – Technical data for measurement equipment [36].

Property	IR Thermometer	Digital Thermometer	Gas analyzer
Measurement range	−30/900 °C	−50/1000 °C	O_2 0–21% CO 100,000 ppm maximum NO_x 4,000 ppm maximum SO_2 4,000 ppm maximum T_{max} 1000 °C
Sensitivity	±2 °C (−30…−5 °C) ±0.75 °C (−4.9…74.9 °C) ±0.75% mv (75…900 °C)	±0.7 °C (−50…900 °C) ±1 °C (900.1…1000 °C)	O_2 ± 2% CO ± 5% NO_x ± 5% SO_2 ± 5% Temperature ± 2 °C
Solution	0.1 °C	0.1 °C (−50…199.9 °C) 1 °C (200…1000 °C)	0.1 °C 1 (for emission measurement)

Supercritical ORC power block

Since the temperature is very high at the outlet of the AHP, there is so much energy waste that can be evaluated by many kinds of processes. However, in the pursuant of the aim of the handled design, the best practice is to generate electricity to power the electrolysis unit which needs it too much to produce O_2 and H_2. By this process, the required energy for PEMEL will not have been met by the electricity generated by the main plant. Therefore, from the national aim of point, both the planned operation of the plant will not be affected and the waste energy will be recovered. For this aim, an ORC cycle was designed to obtain the maximum power from the wastes. The maximum efficiency from an ORC cycle can be obtained when the turbine inlet conditions are set on the points closer to the saturated line of the working fluids [38–40]. In this regard, the selection of the working fluid is another important issue where the physical properties of the cooling fluid (water at this time), the applicable temperature range of the working fluid ($T_{w,min}$ and $T_{w,max}$), the critical temperature (T_{cr}) and pressure (P_{cr}) of the working fluid and of course the environmental issues such as ozone depletion potential (ODP) and global warming potential (GWP) are on the issue. In this study, R601 (pentane) was selected as the most appropriate working fluid. Although the flammability of R601 is higher, R601 can be safely used in a closed system. The properties of R601 are given in Table 4 [41,42].

Since most refrigerant fluids have over-hanged saturated lines, the best choice would be to design the cycle over the critical points if the heat source is appropriate. Therefore, depending on the temperature of the flue gases of the handled unit, the power block was designed as supercritical ORC. The temperature versus entropy change (*T*-*s*) diagram is given in Fig. 2.

According to Fig. 2, the isentropic efficiencies for the pumps and turbine were assumed as 85% where the generator efficiency was taken as 97%. The parasitic losses were taken as 10% of the initial conditions of cycle steps and pressure drops were calculated on this basis at the stage of the design. The heat losses from the surfaces of the heat exchanger were assumed as 2% of the heat energy of the source. The mass, energy, and exergy balances for the supercritical ORC power block are given in Table 5. In the designing stage, the available minimum temperature of flue gases was assumed as 130 °C taking the condensation possibility of SO_2.

Proton exchange membrane electrolyzer-PEMEL

PEMEL is the most common type used for H_2 production depending on its higher efficiency, higher purity of H_2, and higher improvement and commercialization possibility. In the last decades, proton exchange membrane (PEM) cells were combined and PEMEL stacks were formed for larger H_2 production amounts. These kinds of stacks also enable PEM cells to work at higher pressures which results in higher efficiency. The technical properties of the PEMEL stack used in the study are given in Table 6 [43].

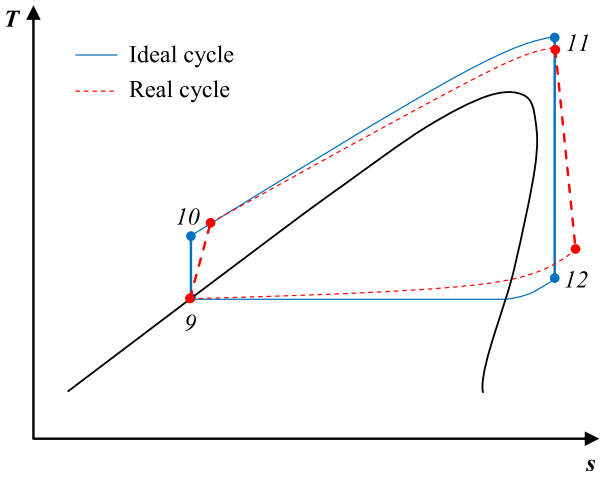

Fig. 2 – *T*-*s* diagram of the proposed supercritical ORC power block.

Taking the properties given in Table 6, the H_2 and O_2 production rates are calculated for the obtained power capacity from the ORC power block. O_2 is used for the enrichment of the combustion air where the use of H_2 is evaluated for two cases. In the first case (Case I), H_2 is stored in a tank as an energy carrier under a pressure of 43,000 kPa offered in Ref [43]. In the second case (Case II), H_2 is fed to the boiler for the enrichment of fuel to obtain a better combustion process [44,45]. The energy and exergy balance equations of the PEMEL group are given in Table 7.

The required power for compressor block ($\dot{W}_{CB}$) is calculated as follows [33]:

$$\dot{W}_C = \dot{m} C_P \frac{T_{19}}{\eta_C}\left[\left(\frac{P_o}{P_i}\right)^{\frac{k-1}{k}} - 1\right] n \quad (21)$$

where the specific heat (C_P), compressor efficiency (η_C), and isentropic exponent (k) C_P, η_C, and k are respectively taken as 14.4 kJ/kg K, 70%, and 1.4. Also, n indicates the number of compression stages and was taken as 5 in this study. The compression ratio was calculated as 1.98 to give the minimum compressor power requirement [33].

Results and discussions

The designed system was evaluated by the energy and exergy analyses method. In this aim, the reference state was taken as

Table 4 – Thermophysical properties of R601 [41,42].

	ODP*	GWP**	P_{cr} (kPa)	T_{cr} (°C)	$T_{w,min}$ (°C)	$T_{w,max}$ (°C)
R601	0	0	3370	196.55	−129.68	326.85

*Relative to R11, ** Relative to CO_2 (100-year time horizon).

Table 5 – Energy and exergy balances for ORC power block.

Compound	Balance Equation	
	Energy	Exergy
P1	$\dot{W}_{P1} = \frac{\dot{m}_9 v(P_{10} - P_9)}{0.85}$	$\dot{E}x_{d,\,P1} = \dot{m}_9(ex_9 - ex_{10}) + \dot{W}_{P1}$
E	$\dot{Q}_E = (\dot{m}_7(h_7 - h_8))0.98 - \dot{m}_{10}(h_{11} - h_{10})$	$\dot{E}x_{d,\,E} = \dot{m}_{10}(h_{11} - h_{10}) - \dot{m}_{10}(ex_{11} - ex_{10}) + \frac{\dot{Q}_E}{T_0}$
T/G	$\dot{W}_T = \dot{m}_{11}(h_{11} - h_{12})0.97$	$\dot{E}x_{d,\,T} = \dot{m}_{12}(ex_{11} - ex_{12}) - \dot{W}_T$
Con	$\dot{Q}_{Con} = (\dot{m}_9(h_9 - h_{12}))0.98 - \dot{m}_{13}(h_{14} - h_{13})$	$\dot{E}x_{d,\,Con} = \dot{m}_9(h_9 - h_{12}) - \dot{m}_{13}(ex_{14} - ex_{13}) + \frac{\dot{Q}_{Con}}{T_0}$

25 °C and 1 atm (1.01 bar). The thermodynamic properties of the reference state for each fluid are given in Table 8.

Combustion process

The handled unit of Seyitömer coal-fired power plant has an installed capacity of 150 MW electricity generation. However, it can not be operated under the design conditions depending on the aging factors since it has a long working period. The current (Base case) status of the unit was measured in-situ [36]. The related values were calculated for all handled cases according to the combustion equation given in Section Boiler group-BG.

In these calculations, the measured values of the boiler parameters such as the generated power, temperature of the points1 to 4, and were kept constant appropriate to the base case for a sensitive comparison. So, the consumed fuel was determined in light of these calculations. The parameters of the combustion process such as the released heat energy ($\dot{Q}_f$), released exergy ($\dot{E}x_f$) and exergy destruction ($\dot{E}x_{d,f}$) rates of combustion process were calculated using the data given in Ref. [46]. The results of the combustion process for each case and the results are given in Table 9. According to Table 9, the released heat energy and exergy of fuel increase depending on the enrichment of combustion air. However, on the contrary to energy and exergy values, the exergy destruction for Case-II is higher than that of Case-I. The main cause of this issue is the additional combustion of H_2 in the boiler. Besides, the base energy (low heating value-LHV) and exergy values were calculated for the efficiency calculations. In this regard, the condensation temperature of the water content in the flue gases was determined for the stoichiometric combustion condition with the standard air. LHV and exergy values of the coal are calculated as 7216.8 and 5824.2 kW/kg-coal, respectively.

Table 6 – Technical characteristics of the PEMEL stack used in the design [43].

Property	Unit	Value
H_2 production	kg/s	0.4414
Capacity	kg H_2/d	1500
Lifetime	h	>60,000
Operating pressure (O_2)	kPa	101.325
Operating pressure (H_2)	kPa	2300
$\dot{W}_{elect}$	kWh/kg H_2	46.6
Current density (J)	A/m^2	15000
Water requirement	kg/s kg H_2	1.59
$\dot{W}_{P2}$	kW/kg H_2	0.3

Results for H_2 production and oxygen-enriched combustion case - Case-I

In Case-I, the generated electricity is 15890.28 kW where 1897.19 kW of this energy is used in the auxiliary components of the PEMEL block and itself. The remained part about 1993.10 kW is used in the PEMEL stack. The produced H_2 and O_2 amounts are 0.0417 and 0.0209 kmol/s, respectively. The thermodynamic properties of Case-I are given in Table 10.

According to the data given in Table 10, energy and exergy analyses was conducted and the results were given in Table 11.

According to Table 11, the highest exergy destruction rate belongs to the boiler group with a value of 261963.72 kW. Evaporator, Turbine, PEM stack, and condenser follows the boiler group with 19561.23, 6047.39, 3720.51, 2386.49 kW in order. The exergy destruction ratios of the components for Case-I are given in Fig. 3.

According to Fig. 3, the exergy destruction of boiler includes the 32.30% of the total exergy inlets to the overall system. In other words, 35.83% of the fuel exergy is destructed by the boiler group (B and APH). The exergy destruction ratio of evaporator, turbine, PEM stack and condenser were recorded as 2.68%, 0.83%, 0.51% and 0.33%, respectively. The total exergy destruction ratio constitutes 67.30% of the exergy inlet of the overall system. The energy and exergy efficiencies of the components and the overall system for Case-I are given in Fig. 4.

According to Fig. 4, the energy and exergy efficiencies of the boiler were obtained as 84.50% and 60.54%, respectively. The energy and exergy efficiencies for the turbine group are orderly 82.45% and 76.47%. For the PEMEL stack, the energy and exergy efficiencies were respectively calculated as 73.94% and 73.41% in conformity of the values of Ref [43]. According to the energy and exergy analyses, the energy and exergy efficiencies of the ORC power block were determined as 15.59% and 32.93%, respectively. For the electrolyzer block, these values were calculated as 67.86% and 66.94% in order.

Table 7 – Energy and exergy balances for the PEMEL group.

Compound	Balance Equation	
	Energy	Exergy
HE	$\dot{Q}_{HE} = (\dot{m}_6(h_6 - h_7))0.98 - \dot{m}_{18}(h_{18} - h_{17})$	$\dot{E}x_{d,HE} = \dot{m}_6(ex_6 - ex_7) - \dot{m}_{18}(ex_{18} - ex_{17}) + \frac{\dot{Q}_{HE}}{T_0}$
PEMEL	$\dot{Q}_{PEMEL} = (\dot{m}_{19}h_{19} + \dot{m}_{32}h_{32} + \dot{m}_{33}h_{33}) - \dot{m}_{16}h_{16} - \dot{W}_T - \dot{W}_{P2}$	$\dot{E}x_{d,PEMEL} = \dot{m}_{16}ex_{16} - (\dot{m}_{19}ex_{19} + \dot{m}_{32}ex_{3222} + \dot{m}_{33}ex_{33}) + \dot{W}_T + \dot{W}_{P2} + \frac{\dot{Q}_{PEMEL}}{T_0}$
P2	$\dot{W}_{P2} = \frac{\dot{m}_{16}v(P_{17} - P_{16})}{0.85}$	$\dot{E}x_{d,\ P2} = \dot{m}_{16}(ex_{17} - ex_{16}) + \dot{W}_{P2}$
CB	$\dot{Q}_{CB} = (\dot{m}_{30}h_{30} + \dot{m}_{48}h_{48}) - (\dot{m}_{19}h_{19} + \dot{m}_{36}h_{36}) - \dot{W}_C$	$\dot{E}x_{d,\ CB} = (\dot{m}_{30}ex_{30} + \dot{m}_{48}ex_{48}) - (\dot{m}_{19}ex_{19} + \dot{m}_{36}ex_{36}) + \dot{W}_C + \frac{\dot{Q}_{CB}}{T_0}$

Table 8 – Thermodynamic properties of the ORC power block.

Point	Fluid	$\dot{m}$ (kg/s) $\dot{n}$ (kmole/s)	T (°C)	P (bar)	h (kJ/kg) h (kJ/kmole)	s (kJ/kg K) s (kJ/kmole K)
0	R-601*	–	25.00	1.01	−25.90	−0.09
	H_2O*	–	25.00	1.01	104.83	0.37
	H_2O	–	25.00	1.01	1886.94	6.61
	H_2	–	25.00	1.01	7863.60	106.75
	O_2	–	25.00	1.01	8672.32	205.03
	Enr. Air	–	25.00	1.01	8662.25	198.55
	Air	–	25.00	1.01	8662.19	198.53

*Values are given for unit kg.

From the point of the overall system, the energy and exergy efficiencies were respectively determined as 25.37% and 31.56%. The energy efficiency increases at a rate of 8.06% in comparison to that of the base case with 23.48%. The increase in exergy efficiency was recorded as 8.49% in comparison to that of the base case with 29.09%.

Results for fuel and oxygen-enriched combustion case - Case-II

In Case-I, the generated electricity is 15834.21 kW where 1312.42 kW of this energy is used in the auxiliary components of the PEMEL block and itself. The remained part about 14521.79 kW is used in the PEMEL stack. The produced H_2 and O_2 amounts are 0.0433 and 0.0216 kmol/s, respectively. The thermodynamic properties of Case-I are given in Table 12.

According to the data given in Table 12, energy and exergy analyses was conducted and the results were given in Table 13.

According to Table 11, the highest exergy destruction rate belongs to the boiler group with a value of 252766.74 kW. Evaporator, Turbine, PEM stack, and condenser follows the boiler group with 19745.81, 6026.05, 3861.08, 2378.07 kW in order. The exergy destruction ratios of the components for Case-I are given in Fig. 5.

According to Fig. 5, the exergy destruction of boiler includes the 31.36% of the total exergy inlets to the overall system. In other words, 34.98% of the fuel exergy is destructed by the boiler group (B and APH). The exergy destruction ratio of evaporator, turbine, PEM stack and condenser were recorded as 2.73%, 0.83%, 0.53% and 0.33%, respectively. The total exergy destruction ratio constitutes 66.70% of the exergy inlet of the overall system. The energy and exergy efficiencies of the components and the overall system for Case-I are given in Fig. 6.

According to Fig. 4, the energy and exergy efficiencies of the boiler were obtained as 84.49% and 61.52%, respectively. The energy and exergy efficiencies for the turbine group are orderly 82.45% and 76.47% as in Case-I. For the PEMEL stack, the energy and exergy efficiencies were respectively calculated as 73.94% and 73.41%. According to the energy and exergy analyses, the energy and exergy efficiencies of the ORC power block were determined as 15.59% and 32.74%, respectively. For the electrolyzer block, these values were calculated as 70.64% and

Table 9 – Technical characteristics of the combustion process and boiler group.

Property	Unit	Base Case	Case- I	Case-II
Fuel Consumption	kg/s	75.21	75.06	73.44
Temperature combustion chamber	°C	1034.20	1038.40	1053.80
Coefficient of excess air (λ)	–	1.680	1.670	1.668
Inlet temperature of flue gases (T_6)	°C	483.00	484.40	489.30
Outlet temperature of flue gases (T_6)	°C	291.10	293.22	296.18
Temperature of combustion air (T_{49})	°C	249.10	251.16	253.07
Released heat energy of fuel ($\dot{Q}_f$)	kW/kg-coal	5059.90	5069.60	5181.40
Released exergy of fuel ($\dot{E}x_f$)	kW/kg-coal	1878.6	1904.7	1995.80
Exergy destruction rate ($\dot{E}x_{d,f}$)	kW/kg-coal	2029.20	2012.4	2021.30
Effectiveness of APH	–	0.49		
Effectiveness of boiler heat exchangers	–	0.68		
Auxiliary power consumption of the handled unit	kW	2567.00		
Net power generation	kW	127433.10		

Table 10 – Thermodynamic properties of Case-I.

Point	Fluid	$\dot{m}$ (kg/s) $\dot{n}$ (kmole/s)	T (°C)	P (bar)	h (kJ/kg) $\bar{h}$ (kJ/kmole)	s (kJ/kg K) $\bar{s}$ ((kJ/kmole K)
1	H_2O*	131.90	220.00	157.31	943.55	943.55
2	H_2O*	120.50	349.00	34.32	3103.91	3103.91
3	H_2O*	131.90	538.00	137.29	3430.98	3430.98
4	H_2O*	120.50	538.00	33.83	3539.18	3539.18
5	Flue gases**	–	484.36	–	−8535.89	−8535.89
6	Flue gases**	–	293.22	–	−10053.31	−10053.31
7	Flue gases**	–	292.92	–	−10055.65	−10055.65
8	Flue gases**	–	130.00	–	−11300.97	−11300.97
9	R-601*	142.1075	27.00	0.74	−21.28	−21.28
10	R-601*	142.1075	31.15	44.44	−7.94	−7.94
11	R-601*	142.1075	220.00	40.00	636.71	636.71
12	R-601*	142.1075	110.90	0.82	501.09	501.09
13	H_2O*	1581.3198	20.00	1.77	83.92	83.92
14	H_2O*	1581.3198	31.00	1.37	129.92	129.92
15	H_2O	0.0417	25.00	1.01	1886.94	1886.94
16	H_2O	0.0621	43.08	1.01	3247.47	3247.47
17	H_2O	0.0621	43.13	1.25	3251.15	3251.15
18	H_2O	0.0621	80.00	1.13	6030.36	6030.36
19	H_2	0.0417	80.00	23.00	9470.00	9470.00
20	H_2	0.0417	40.00	23.00	8314.40	8314.40
21	H_2	0.0417	108.12	45.54	11111.40	11111.40
22	H_2	0.0417	40.00	45.54	8335.60	8335.60
23	H_2	0.0417	108.12	90.17	10368.80	10368.80
24	H_2	0.0417	40.00	90.17	8382.80	8382.80
25	H_2	0.0417	108.12	178.55	10485.40	10485.40
26	H_2	0.0417	40.00	178.55	8483.20	8483.20
27	H_2	0.0417	108.12	353.53	10732.20	10732.20
28	H_2	0.0417	40.00	353.53	8709.40	8709.40
29	H_2	0.0417	108.12	700.00	11257.40	11257.40
30	H_2	0.0417	40.00	700.00	9214.40	9214.40
31	H_2O/O_2	–	80.00	1.01	–	–
32	H_2O	0.0204	80.00	1.01	6030.36	6030.36
33	O_2	0.0209	80.00	1.01	10299.20	10299.20
34	Air	16.4848	25.00	1.01	8662.19	8662.19
35	O_2	0.0209	80.00	1.01	10299.20	10299.20
36	Enriched air	16.4086	26.80	1.01	8715.56	8715.56
37	Enriched air	16.4086	26.90	1.01	8718.44	8718.44
38	Enriched air	3.2817	26.90	1.01	8718.44	8718.44
39	Enriched air	3.2817	28.09	1.01	8753.01	8753.01
40	Enriched air	3.2817	26.90	1.01	8718.44	8718.44
41	Enriched air	3.2817	27.75	1.01	8743.17	8743.17
42	Enriched air	3.2817	26.90	1.01	8718.44	8718.44
43	Enriched air	3.2817	27.76	1.01	8743.37	8743.37

Table 10 – (continued)

Point	Fluid	$\dot{m}$ (kg/s) $\dot{n}$ (kmole/s)	T (°C)	P (bar)	h (kJ/kg) $\overline{h}$ (kJ/kmole)	s (kJ/kg K) $\overline{s}$ ((kJ/kmole K)
44	Enriched air	3.2817	26.90	1.01	8718.44	8718.44
45	Enriched air	3.2817	27.76	1.01	8743.63	8743.63
46	Enriched air	3.2817	26.90	1.01	8718.44	8718.44
47	Enriched air	3.2817	27.77	1.01	8743.88	8743.88
48	Enriched air	16.4086	27.82	1.01	8745.41	8745.41
49	Enriched air	16.4086	251.16	1.01	15340.58	15340.58

*Values are given in per kg, **$\overline{h}$ values are given in $\Delta\overline{h} = \overline{h} - \overline{h}_0$.

Table 11 – Energy and exergy analysis results for Case-I.

Component	$\dot{E}_i$ (kW)	$\dot{E}_o$ (kW)	$\dot{Q}$ (kW)	$\dot{W}$ (kW)	$\dot{E}x_i$ (kW)	$\dot{E}x_o$ (kW)	$\dot{E}x_d$ (kW)
B	1040197.35	879017.90	161179.45	–	598444.87	362270.59	236174.28
APH	113903.35	108217.14	−5686.21	–	53956.33	28147.81	25789.44
E	93478.51	91608.94	−1869.57	–	44254.67	24687.17	19561.23
Con	74233.28	72748.62	−1484.67	74.71	4668.76	2361.97	2386.49
P1	17.83	1073.59	−186.31	1242.08	17.83	1073.59	186.94
T	90481.29	71208.67	−3382.35	15890.28	25698.19	3749.16	6047.39
PEM	374.45	10347.09	−4020.46	13993.10	21.33	10280.43	3720.51
CB	143404.65	143883.85	−681.06	580.13	12302.37	12701.32	178.89
HE-I	176.01	172.57	−3.43	–	129.46	18.77	110.68
P2	201.65	201.88	−0.04	0.26	2.55	2.56	0.25
M	143009.69	143009.69	0.00	–	2214.34	2132.90	81.44
Overall system	541722.43	140009.45	−178493.55	127433.07	437188.20	140558.18	294237.54

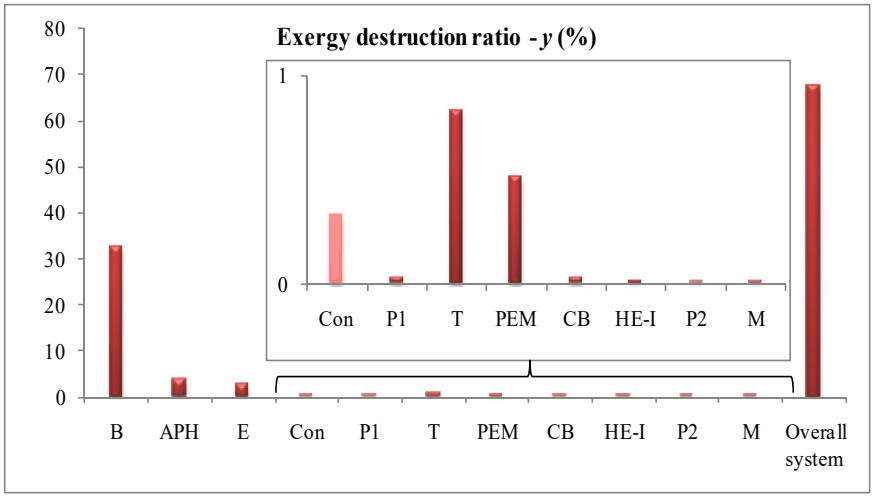

Fig. 3 – Exergy destruction ratios of the components for Case-I.

69.69% in order. From the point of the overall system, the energy and exergy efficiencies were respectively determined as 24.05% and 29.80%. The energy efficiency increases at a rate of 2.45% in comparison to that of the base case with 23.48%. The increase in exergy efficiency was also recorded as 2.45% in comparison to that of the base case with 29.09%.

Additionally, if the single ORC power block is taken into consideration for the recovery of waste heat, the increase in energy and exergy efficiency of the overall system would be recorded as 11.47% with an energy efficiency of 26.15% and an exergy efficiency of 32.40%. Although the single ORC power block addition gives a more efficient result, it has no impact on

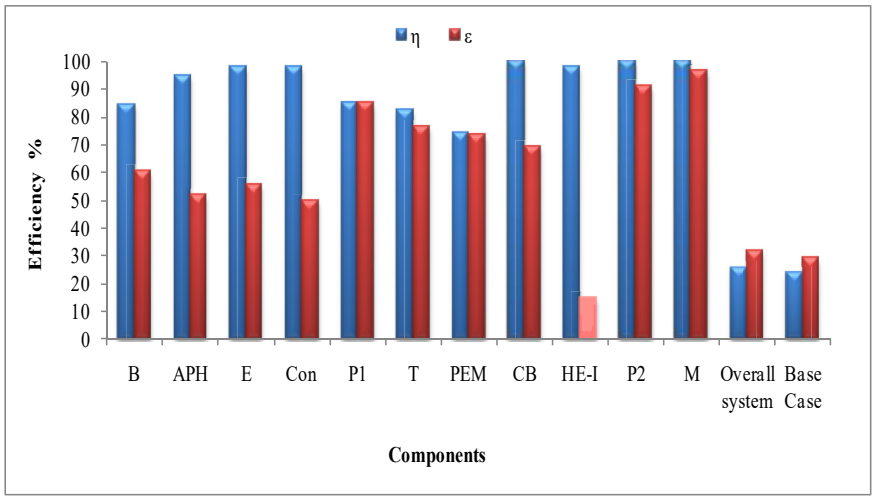

Fig. 4 – Energy and exergy efficiencies of the components for Case-I.

the emission reduction and combustion improvement from the environmental side of the point.

Environmental evaluation

In case-I, in which just the combustion air is enriched with the O_2 product of PEMEL and the other product H_2 is stored as an energy carrier, the benefit from the coal consumption is about 0.2% with a CO_2 reduction of 40,275.20 kg per year. In Case-II, in which both the combustion air and fuel are enriched, the benefit from the coal consumption is about 2.35% with a CO_2 reduction of 506,250.27 kg per year. The values of reduced emissions are given in Table 14.

Table 12 – Thermodynamic properties of Case-II.

Point	Fluid	$\dot{m}$ (kg/s) $\dot{n}$ (kmole/s)	T (°C)	P (bar)	h (kJ/kg) $\overline{h}$ (kJ/kmole)	s (kJ/kg K) $\overline{s}$ ((kJ/kmole K)
1	H_2O*	131.90	220.00	157.31	131.90	220.00
2	H_2O*	120.50	349.00	34.32	120.50	349.00
3	H_2O*	131.90	538.00	137.29	131.90	538.00
4	H_2O*	120.50	538.00	33.83	120.50	538.00
5	Flue gases**	–	489.32	–	–	489.32
6	Flue gases**	–	296.18	–	–	296.18
7	Flue gases**	–	295.86	–	–	295.86
8	Flue gases**	–	130.00	–	–	130.00
9	R-601*	141.6061	27.00	0.74	141.6061	27.00
10	R-601*	141.6061	31.15	44.44	141.6061	31.15
11	R-601*	141.6061	220.00	40.00	141.6061	220.00
12	R-601*	141.6061	110.90	0.82	141.6061	110.90
13	H_2O*	1575.7401	20.00	1.77	1575.7401	20.00
14	H_2O*	1575.7401	31.00	1.37	1575.7401	31.00
15	H_2O	0.0433	25.00	1.01	0.0433	25.00
16	H_2O	0.0644	43.08	1.01	0.0644	43.08
17	H_2O	0.0644	43.13	1.25	0.0644	43.13
18	H_2O	0.0644	80.00	1.13	0.0644	80.00
19	H_2	0.0433	80.00	23.00	0.0433	80.00
31	H_2O/O_2	–	80.00	1.01	–	80.00
32	H_2O	0.0212	80.00	1.01	0.0212	80.00
33	O_2	0.0216	80.00	1.01	0.0216	80.00
34	Air	16.1218	25.00	1.01	16.1218	25.00
35	O_2	0.0216	80.00	1.01	0.0216	80.00
36	Enriched air	16.0302	27.16	1.01	16.0302	27.16
49	Enriched air	16.0302	253.25	1.01	16.0302	253.25

*Values are given in per kg, **$\overline{h}$ values are given in $\Delta\overline{h} = \overline{h} - \overline{h}_0$.

Table 13 – Energy and exergy analysis results for Case-II.

Component	$\dot{E}_i$ (kW)	$\dot{E}_o$ (kW)	$\dot{Q}$ (kW)	$\dot{W}$ (kW)	$\dot{E}x_i$ (kW)	$\dot{E}x_o$ (kW)	$\dot{E}x_d$ (kW)
B	1028266.77	879017.90	−149248.86	–	588816.49	362230.56	226585.93
APH	112748.98	106041.65	−6707.33	–	53718.10	27514.78	26180.81
E	93148.67	91285.70	−1862.97	–	44352.13	24600.06	19745.81
Con	73971.35	72491.92	−1479.43	74.45	4652.29	2353.63	2378.07
P1	17.76	1069.81	−185.65	1237.70	17.76	1069.81	186.28
T	90162.03	70957.41	−3370.41	15834.21	25607.51	3735.94	6026.05
PEM	388.60	10738.03	−4172.37	14521.79	22.14	10668.86	3861.08
HE-I	182.92	179.09	−3.83	–	134.20	19.48	114.70
P2	209.27	209.50	−0.04	0.27	2.64	2.66	0.26
M	139872.97	139872.97	0.00	–	2170.69	2078.00	92.69
Overall system	529791.85	130000.08	−167030.89	127433.07	427559.82	127433.07	285171.68

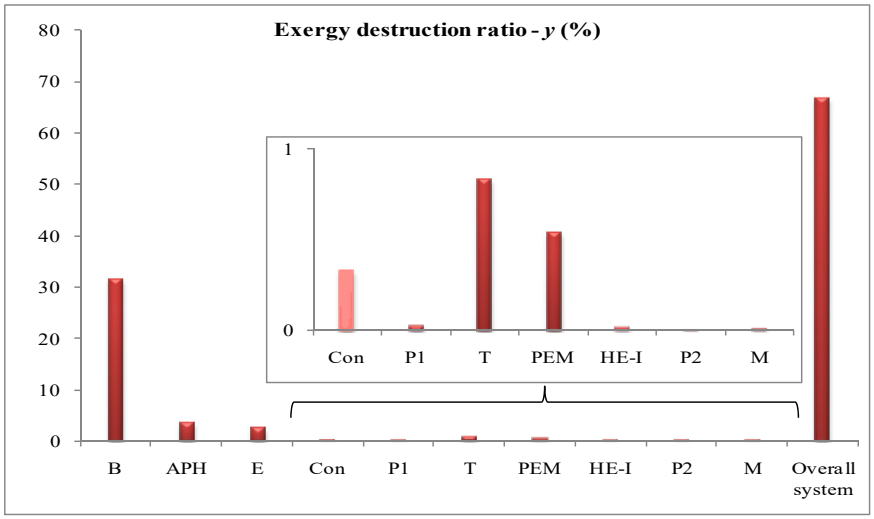

Fig. 5 – Exergy destruction ratios of the components for Case-II.

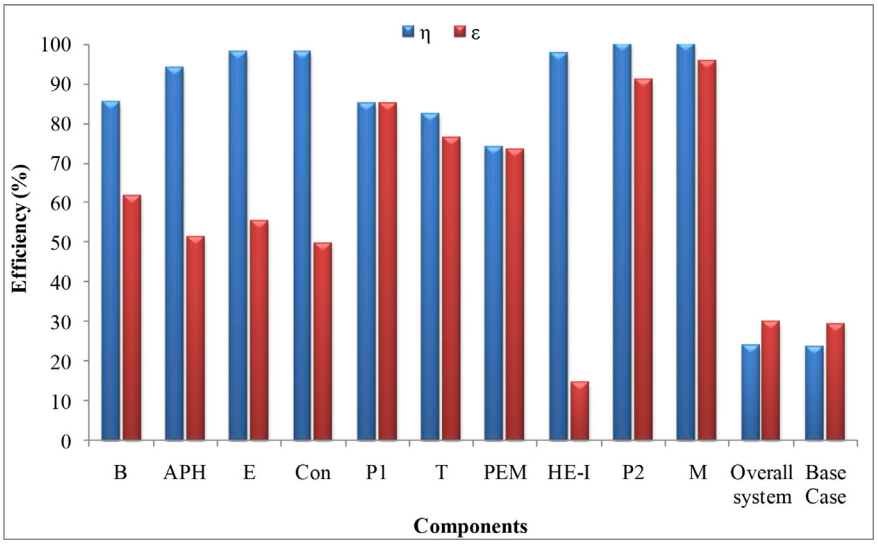

Fig. 6 – Energy and exergy efficiencies of the components for Case-II.

Table 14 – Emission reduction (kg/y).

Emission	Case-I	Case-II
CO_2	40,275.20	506,250.27
CO	1,875.86	23,579.17
NO_2	44.53	559.72
SO_2	629.85	7,917.02
Fuel	3,703,625.12	46,553,739.21

Conclusions

A multi-generation system was designed for the waste recovery of a 150 MW coal-fired power plant. In this regard, the waste heat from the boiler system of the power plant is recycled in the supercritical ORC power block to obtain the required energy for the PEMEL block. Then, two different cases were handled to utilize the products of the PEMEL block. In the first case (Case-I), H_2 was stored as an energy carrier to be used for external operations where O_2 was used for the enrichment of the combustion air. In the second case (Case-II), H_2 was used for the enrichment of the fuel where O_2 was used for the enrichment of the combustion air as in the first case. Finally, the observed cases were analyzed by energy and exergy methods. The H_2 and O_2 production amounts were respectively calculated as 0.0417 and 0.0209 kmol/s for Case-I where these amounts were respectively calculated as 0.0433 and 0.0216 kmol/s for Case-II. The energy efficiency of the overall system was determined as 25.37% and 24.05% for Case-I and Case-II, respectively. The exergy efficiency of the overall system was determined as 31.56% and 29.80% for Case-I and Case-II, respectively. The energy efficiency of the overall system increase by about 8.06% and 2.45% for Case-I and Case-II, respectively. The exergy efficiency of the overall system increase by about 8.49% and 2.45% for Case-I and Case-II, respectively. The CO_2 emission reduction is 40,275.20 and 506,250.27 kg/y for Case-I and Case-II, respectively. The fuel-saving is 3,703,625.12 and 46,553,739.21 kg/y for Case-I and Case-II, respectively.

Declaration of competing interest

The authors declare that they have no known competing financial interests or personal relationships that could have appeared to influence the work reported in this paper.

Nomenclature

$\dot{E}$	energy rate (kW)
ex	specific flow exergy (kJ/kg)
$\dot{E}x$	exergy rate (kW)
h	specific enthalpy (kJ/kg)
$\overline{h}$	specific molar enthalpy (kJ/kmole)
I	exergy destruction rate (kW)
$\dot{m}$	mass flow rate (kg/s)
$\dot{n}$	molar rate (kmole/s)
P	Pressure (kPa, bar, or atm)
$\dot{Q}$	heat rate (kW)
R_u	universal gas constant (kJ/kmole K)
s	specific entropy (kW/kg K)
T	temperature (K or °C)
$\dot{W}$	work rate (kW)
x	molar fraction
y	exergy destruction ratio

Greek symbols

ε	exergy efficiency (%)
η	energy efficiency (%)
λ	coefficient of excess air

Subscripts

cc	combustion chamber
d	destruction
f	fuel
g	generated
i	inlet or ith component
k	kth component
o	outlet
p	product or reactant
s	isentropic
T	value at a specified temperature
0	value at the reference state

Superscripts

ch	chemical
f	formation
ph	physical
Q	exergy term related to heat
W	exergy term related to work
o	standard

Abbreviations

AEL	alkaline electrolyzer
APH	air preheater
B	boiler
BG	boiler group
C	compressor
CB	compressor block
Con	condenser
HE	heat exchanger
HTEL	high-temperature electrolyzer
ORC	organic Rankine cycle
P	pump
PEM	proton exchange membrane
PEMEL	proton exchange membrane electrolyzer
T	turbine group

REFERENCES

[1] RTMEN (Republic of Turkey Ministry of Energy and Natural Resources). Data for electricity generation in Turkey. 2020. Available from: https://www.enerji.gov.tr/en-US/Pages/Electricity (Last Access: April 2020).

[2] Arslan O, Acar MS. Enhanced exergetic evaluation of regenerative and recuperative coal-fired power plant. Int J Exergy 2020. In press.

[3] Gao J, Zhang Q, Wang X, Song D, Liu W, Liu W. Exergy and exergoeconomic analyses with modeling for CO_2 allocation of coal-fired CHP plants. Energy 2018;152:562–75.

[4] Yang Y, Wang L, Dong C, Xu G, Morosuk T, Tsatsaronis G. Comprehensive exergy-based evaluation and parametric study of a coal-fired ultra-supercritical power plant. Appl Energy 2013;112:1087–99.
[5] Madejski P. Numerical study of a large-scale pulverized coal-fired boiler operation using CFD modeling based on the probability density function method. Appl Therm Eng 2018;145:352–63.
[6] Madejski P, Zymelka P. Calculation methods of steam boiler operation factors under varying operating conditions with the use of computational thermodynamic modeling. Energy 2020;197:117221.
[7] Shi Y, Liu Q, Shao Y, Zhong W. Energy and exergy analysis of oxy-fuel combustion based on circulating fluidized bed power plant firing coal, lignite and biomass. Fuel 2020;269:117424.
[8] Bisioa G, Bosio A, Rubatto G. Thermodynamics applied to oxygen enrichment of combustion air. Energy Convers Manag 2002;43:2589–600.
[9] Yin C, Yan J. Oxy-fuel combustion of pulverized fuels: combustion fundamentals and modeling. Appl Energy 2016;162:742–62.
[10] Baukal CE. Oxygen-enhanced combustion. United States: CRC Press LLC; 1998.
[11] Horbaniuc B, Marin O, Dumitrascu G, Charon O. Oxygen-enriched combustion in supercritical steam boilers. Energy 2004;29:427–48.
[12] Tiwari HP, Das A, Singh U. Novel technique for assessing the burnout potential of pulverized coals/coal blends for blast furnace injection. Appl Therm Eng 2018;130:1279–89.
[13] Zhou A, Xu H, Tu Y, Zhao F, Zheng Z, Yang W. Numerical investigation of the effect of air supply and oxygen enrichment on the biomass combustion in the grate boiler. Appl Therm Eng 2019;156:550–61.
[14] Yu Z, Ma X, Liao Y. Mathematical modeling of combustion in a grate-fired boiler burning straw and effect of operating conditions under air- and oxygen-enriched atmospheres. Renew Energy 2010;35:895–903.
[15] Smolinka T, Ojong ET, Garche J. Hydrogen production from renewable energies-electrolyzer technologies. In: Moseley PY, Garche J, editors. Electrochemical energy storage for renewable sources and grid balancing. Elsevier B.V.; 2015. p. 103–28.
[16] Ishaq H, Dincer I, Naterer GF. Performance investigation of an integrated wind energy system for co-generation of power and hydrogen. Int J Hydrogen Energy 2018;43:9153–64.
[17] Bicer Y, Dincer I. Development of a new solar and geothermal based combined system for hydrogen production. Sol Energy 2016;127:269–84.
[18] Bamisile O, Huang Q, Dagbasi M, Kemena AD. Performance analysis of a novel solar PTC integrated system for multi-generation with hydrogen production. Int J Hydrogen Energy 2020;45:190–206.
[19] Safari F, Dincer I. Assessment and optimization of an integrated wind power system for hydrogen and methane production. Energy Convers Manag 2018;177:693–703.
[20] Balta MT, Dincer I, Hepbasli A. Thermodynamic assessment of geothermal energy use in hydrogen production. Int J Hydrogen Energy 2009;34:2925–39.
[21] Omar MA, Altinisik K. Simulation of hydrogen production system with hybrid solar collector. Int J Hydrogen Energy 2016;41:12836–41.
[22] Seyitoglu SS, Dincer I, Kilicarslan A. Energy and exergy analyses of hydrogen production by coal gasification. Int J Hydrogen Energy 2017;42:2592–600.
[23] Gokcek M, Kale C. Techno-economical evaluation of a hydrogen refuelling station powered by Wind-PV hybrid power system: a case study for Izmir-Cesme. Int J Hydrogen Energy 2018;43:10615–25.
[24] Yilmaz F, Ozturk M, Selbas R. Thermodynamic investigation of a concentrating solar collector based combined plant for poly-generation. Int J Hydrogen Energy 2020;45:26138–55.
[25] Fereidooni M, Mostafaeipour A, Kalantar V, Goudarzi H. A comprehensive evaluation of hydrogen production from photovoltaic power station. Renew Sustain Energy Rev 2018;82:415–23.
[26] Mohamed WANW, Kamil MHM. Hydrogen preheating through waste heat recovery of an open-cathode PEM fuel cell leading to power output improvement. Energy Convers Manag 2016;124:543–55.
[27] Hasani M, Rahba N. Application of thermoelectric cooler as a power generator in waste heat recovery from a PEM fuel cell – an experimental study. Int J Hydrogen Energy 2015;40(43):15040–51.
[28] Khanmohammadi S, Saadat-Targhi M, Ahmed FW, Afrand M. Potential of thermoelectric waste heat recovery in a combined geothermal, fuel cell and organic Rankine flash cycle (thermodynamic and economic evaluation). Int J Hydrogen Energy 2020;45:6934–48.
[29] Lummen N, Karouach A, Tveitan S. Thermo-economic study of waste heat recovery from condensing steam for hydrogen production by PEM electrolysis. Energy Convers Manag 2019;185:21–34.
[30] Nami H, Mohammadkhani F, Ranjbar F. Utilization of waste heat from GTMHR for hydrogen generation via combination of organic Rankine cycles and PEM electrolysis. Energy Convers Manag 2016;127:589–98.
[31] Feili M, Rostamzadeh H, Parikhani T, Ghaebi H. Hydrogen extraction from a new integrated trigeneration system working with zeotropic mixture, using waste heat of a marine diesel engine. Int J Hydrogen Energy 2020;45:21969–94.
[32] Thiyagarajan S, Sonthalia A, Geo VE, Chokkalingam B. Effect of waste exhaust heat on hydrogen production and its utilization in CI engine. Int J Hydrogen Energy 2020;45:5987–96.
[33] Cengel YA, Boles MA. Thermodynamics: an engineering approach. New York. USA: McGraw Hill Inc.; 1994.
[34] Bejan A, Tsatsaronis G, Moran M. Thermal design and optimization. New York. USA: John Wiley & Sons Inc.; 1996.
[35] Acar MS, Saraydar M, Arslan O. Exergetical evaluation of lignite production process: SLI case study. J Polytech 2018;21:55–63.
[36] Arslan O. reportThe first and second law analysis of Seyitomer coal-fired power plant. M.Sc. Thesis, Institute of Applied Sciences, Dumlupinar University, Turkey, 05205.
[37] Arslan O, Ozgur MA, Yildizay HD, Kose R. Fuel effects on optimum insulation thickness: an exergetic approach. Energy Sources, Part A Recovery, Util Environ Eff 2010;32:128–47.
[38] Arslan O, Ozgur MA, Kose R. Electricity generation ability of the Simav geothermal field: a technoeconomic approach. Energy Sources, Part A Recovery, Util Environ Eff 2012;34(12):1130–44.
[39] Arslan O, Yetik O. ANN modeling of an ORC-binary geothermal power plant: simav case study. Energy Sources, Part A Recovery, Util Environ Eff 2014;36(4):418–28.
[40] Arslan O, Yetik O. ANN based optimization of supercritical ORC-Binary geothermal power plant: simav case study. Appl Therm Eng 2011;31(17–18):3922–8.
[41] Restrepo G, Weckert M, Bruggemanns R, Gerstmann S, Frank H. Ranking of refrigerants. Environ Sci Technol 2008;42(8):2925–30.

[42] REFPROP. Reference Fluid thermodynamic and transport properties. NIST reference database. Version 9.0. National Insitiute of Standards and Technology, U.S.A; 2010.
[43] Hamdan M. PEM electrolyzer incorporating an advanced low cost membrane. Final scientific and technical report of the project under grant No. DE-FG36-08GO18065. U.S. Department of Energy; 2013.
[44] Pisa I, Lazaroiu G, Prisecaru T. Influence of hydrogen enriched gas injection upon polluting emissions from pulverized coal combustion. Int J Hydrogen Energy 2014;39:17702–9.
[45] Schiro F, Stoppato A, Benato A. Modelling and analyzing the impact of hydrogen enriched natural gas on domestic gas boilers in a decarbonization perspective. Carbon Resour Convers 2020;3:122–3.
[46] Strehlow RA. Combustion fundamentals. In: Energy, combustion and environment series. Singapore. Singapore: McGraw Hill Inc.; 1984.